Mathematics

http://www.aimspress.com/journal/Math

AIMS Mathematics, 11(7): 20143–20169.
DOI: 10.3934/math.2026818
Received: 30 April 2026
Revised: 28 June 2026
Accepted: 01 July 2026
Published: 09 July 2026

Research article

Mathematical and computational analysis of a Kayo-Kengne-Akgül fractional-order Lassa fever model

Ramsha Shafqat[1,*] and Mohammed M. Alshamrani[2]

[1] Department of Mathematics and Statistics, The University of Lahore, Sargodha 40100, Pakistan
[2] Department of Mathematics and Statistics, College of Science, Taif University, P.O. Box 11099, Taif 21944, Saudi Arabia

* **Correspondence:** Email: ramshawarriach@gmail.com.

Abstract: This study developed a Caputo-type Kayo-Kengne-Akgül (KKA) fractional model for Lassa fever transmission with memory in coupled human-rodent dynamics. The model contains five compartments: susceptible, infected, and recovered humans, together with susceptible and infected rodents. Using the inverse relation between the KKA derivative and its associated integral, the system was rewritten as an equivalent Volterra-type integral equation. The analysis proved positivity, boundedness, existence, uniqueness, and Ulam-Hyers stability. For computation, a two-step KKA Adams-Bashforth scheme was constructed to examine the effect of the fractional order, showing that smaller orders produce stronger memory and slower epidemic evolution. A deep neural network surrogate was trained on the numerical trajectories, and parameter estimation from clean and noisy synthetic data showed close agreement between the reference and recovered solutions for all compartments and selected transmission parameters.

Keywords: Lassa fever; Kayo-Kengne-Akgül derivative; fractional-order epidemic model; existence and uniqueness; Ulam-Hyers stability; Adams-Bashforth scheme
Mathematics Subject Classification: 34D20, 34K20, 34K60, 92C60, 92D45

1. Introduction

Lassa fever remains an important zoonotic disease in several parts of West Africa, with Nigeria bearing a particularly heavy burden. It was first recognized in 1969 after the deaths of two missionary nurses from a severe febrile infection. Subsequent research identified the causative agent as Lassa virus (LASV), an RNA virus belonging to the family Arenaviridae [1]. The infection is maintained in nature primarily through the Mastomys rodent reservoir. Human transmission usually occurs through contact with food, surfaces, or other materials contaminated by rodent urine or feces, while person-to-person spread may also occur through exposure to the bodily fluids of an infected individual. Although many infections are mild or asymptomatic, severe cases may lead to hemorrhage, respiratory distress, multi-organ failure, neurological complications, and death. The disease is particularly dangerous for pregnant women and hospitalized patients, making it an important subject for epidemiological analysis [2].

The persistence of Lassa fever in endemic regions shows that its transmission dynamics are influenced by several interacting mechanisms, including human-rodent contact, secondary human-to-human transmission, delayed diagnosis, and variability in treatment and control measures. These epidemiological features make Lassa fever a suitable candidate for mathematical modeling. Mathematical models help to identify the main transmission pathways, evaluate the role of key parameters, determine threshold conditions for disease persistence or eradication, and assess the possible effects of intervention strategies. In this way, modeling provides a useful theoretical framework for understanding disease spread and supporting public-health decision-making.

Several key factors influence the transmission potential of Lassa fever. These include the frequency of contact between humans and infected rodents, the level of environmental contamination by rodent urine or feces, secondary human-to-human transmission, the size of the susceptible human population, the abundance and infection level of the rodent reservoir, recovery and treatment rates, disease-induced mortality, waning immunity, and natural demographic processes. In addition, delayed diagnosis and repeated exposure may affect the timing and intensity of disease progression. These mechanisms are reflected in the model through the human-to-human transmission rate, rodent-to-human transmission rate, human-to-rodent transmission rate, recruitment rates, recovery rate, waning-immunity rate, natural mortality rates, disease-induced death rate, and the fractional order controlling memory effects.

The mathematical modeling literature on Lassa fever has grown steadily in recent years. Early and recent studies include deterministic compartmental models that describe disease spread between humans and rodents while analyzing the behavior of disease-free and endemic equilibria [1, 3]. Researchers have also proposed time-dependent models to capture seasonal changes in rodent populations and to evaluate the impact of different intervention policies on transmission patterns [4]. In a related direction, optimal-control approaches have been applied to assess how hospitalization, treatment, health education, and rodent management can work together to reduce infection levels [5, 6].

Additional studies have addressed treatment adherence, parameter sensitivity, and mathematical conditions for equilibrium stability in both local and global settings [7, 8]. This body of work has deepened the theoretical understanding of Lassa fever spread and control.

Despite these important contributions, most existing Lassa fever models are still formulated in the classical integer-order setting. In many epidemiological processes, however, the present disease state may depend not only on current interactions but also on past exposure, delayed biological response, and earlier stages of infection. Such hereditary effects are difficult to represent adequately within standard integer-order models. Fractional-order modeling provides a natural extension by incorporating memory into the governing dynamics, and operators with nonlocal kernels have therefore become increasingly useful in epidemic modeling when past states influence current transmission behavior.

The main novelty of the present study lies in extending Lassa fever transmission modeling from the classical integer-order setting to the Caputo-type KKA fractional-order framework. Classical models usually describe the rate of change of each compartment only in terms of the current state of the system. However, Lassa fever transmission may be influenced by previous exposure history, repeated human-rodent contact, delayed diagnosis, and persistence of infection within the reservoir population. These features motivate the use of a fractional-order formulation, since the fractional derivative incorporates memory effects through a nonlocal temporal structure. In this sense, the fractional order acts as an additional modeling parameter that controls the strength of memory and allows the model to describe slower, smoother, and more realistic transient epidemic behavior. Moreover, the use of the Caputo-type KKA operator is new in this context and provides a convenient integral representation for rigorous analysis and numerical approximation. It should be noted that the proposed model can reduce to the classical integer-order formulation when $\alpha = 1$. Therefore, the integer-order model is not excluded; rather, it is contained as a limiting case of the present fractional-order framework. The main reason for considering $0 < \alpha < 1$ is that Lassa fever transmission is not necessarily governed only by the current epidemiological state. Previous exposure, repeated contact with infected rodents, delayed clinical response, and persistence of infection in the reservoir population may influence the present disease dynamics. The fractional-order derivative provides a convenient way to incorporate these memory-dependent effects, while the parameter α allows the strength of memory to be varied and examined numerically.

Motivated by this observation, the present work investigates a fractional-order Lassa fever model in the Caputo-type KKA framework. The KKA operator is particularly attractive because it incorporates memory effects while preserving a convenient inverse relation with its associated fractional integral. This feature allows the governing system to be reformulated as an equivalent Volterra-type integral equation, which provides a suitable foundation for rigorous qualitative analysis as well as numerical approximation. In addition, the KKA formulation offers extra flexibility in describing the transient dynamics of the coupled human-rodent transmission process when compared with the classical first-order model.

Recent studies have further shown the effectiveness of fractional-order frameworks in modeling infectious and biological disease dynamics under different analytical, numerical, and control settings. For instance, El-Mesady et al. [9] investigated optimal control efforts for reducing Human Papillomavirus transmission using a fractional-order mathematical model, while Elsonbaty et al. [10] developed a fractional-order meningitis model with optimal control strategies to describe infection dynamics and intervention effects. In addition, Shafqat and Alshamrani [11] employed deep learning for parameter estimation in a typhoid fever model, and Shafqat and Alsaadi [12] proposed a hybrid predictive framework for Zika dynamics based on the normalized Caputo-Fabrizio operator. Further contributions include the normalized Caputo-Fabrizio fractional model for ischemic heart disease progression with well-posedness and Ulam-Hyers stability analysis by Al-Quran et al. [13], and the SVIR fractional modeling and bifurcation analysis presented by Shafqat et al. [14]. These studies confirm the growing importance of fractional operators, stability analysis, optimal control, bifurcation theory, and data-driven techniques in modern disease modeling, and they further motivate the present KKA fractional-order formulation for Lassa fever dynamics.

The novelty and main contributions of this work are summarized as follows. First, to the best of our knowledge, this is the first study to formulate Lassa fever transmission dynamics within the Caputo-type KKA fractional-order framework. Second, the model incorporates memory effects into the coupled human-rodent transmission process, which cannot be adequately represented by a purely integer-order formulation. Third, the inverse relation between the KKA derivative and its associated integral is used to obtain an equivalent Volterra-type integral system, which provides the basis for proving positivity, boundedness, existence, uniqueness, and Ulam-Hyers stability. Fourth, a two-step KKA Adams-Bashforth numerical scheme is derived to investigate the influence of the fractional order on disease progression. Finally, a deep neural network surrogate and parameter-estimation procedure are developed to support the computational and predictive aspects of the proposed model.

The paper is structured in the following way. Section 2 describes the fractional-order Lassa fever model and establishes its main qualitative properties. In Section 3, we review the basic concepts associated with the KKA operator. Section 4 is concerned with the development of the Adams-Bashforth numerical procedure. The computational results and their discussion, together with the deep neural network surrogate analysis, are presented in Section 5. The parameter-estimation framework is then examined in Section 6. Finally, section 7 concludes the paper with a summary of the main results and several suggestions for future research.

2. Model formulation

In this study, we formulate a fractional-order model for the transmission dynamics of Lassa fever by employing the KKA operator. Because the disease is sustained through coupled interactions between the human population and the rodent reservoir, it is desirable to use a framework that can account for both transmission coupling and memory effects. Accordingly, the classical first-order derivative is replaced with the KKA fractional derivative of order $0 < \alpha \leq 1$. When $\alpha = 1$, the system reduces to the corresponding classical integer-order Lassa fever model, whereas the case $0 < \alpha < 1$ represents the memory-dependent fractional extension considered in this work.

At time t, the human population is divided into three compartments, namely, susceptible, infected, and recovered individuals, denoted by $S(t)$, $I(t)$, and $R(t)$, respectively. In the same way, the rodent population is partitioned into susceptible and infected classes, represented by $M(t)$ and $J(t)$. Hence, the total human and rodent populations are given by $N_h(t) = S(t) + I(t) + R(t)$ and $N_r(t) = M(t) + J(t)$.

The susceptible human population is recruited into the model at rate Λ_h, whereas susceptible rodents are added at rate Λ_r. Infection in humans is assumed to occur through effective contact with either infected humans or infected rodents. The corresponding transmission coefficients are denoted by β_h and β_r, respectively. Under these assumptions, the force of infection for the human population is given by

$$\lambda_h(t) = \frac{\beta_h I(t) + \beta_r J(t)}{N_h(t)}.$$

In an analogous manner, rodents are assumed to contract infection through effective exposure to infected humans, governed by the parameter β_{hr}. This leads to the rodent infection pressure

$$\lambda_r(t) = \frac{\beta_{hr} I(t)}{N_r(t)}.$$

In the infected human compartment, recovery takes place at rate ε, while individuals in the recovered class may lose their temporary immunity and move back to the susceptible class at rate γ. Disease-related death among infected humans is represented by the parameter δ_h. In addition, natural death is assumed in both the human and rodent populations, occurring at rates μ_h and μ_r, respectively. Based on these modeling assumptions, the KKA fractional-order system for Lassa fever can be written as follows:

$$\begin{cases} {}^{KKA}D_t^{\alpha}S(t) = \Lambda_h + \gamma R(t) - \lambda_h(t)S(t) - \mu_h S(t), \\ {}^{KKA}D_t^{\alpha}I(t) = \lambda_h(t)S(t) - (\varepsilon + \mu_h + \delta_h)I(t), \\ {}^{KKA}D_t^{\alpha}R(t) = \varepsilon I(t) - (\mu_h + \gamma)R(t), \\ {}^{KKA}D_t^{\alpha}M(t) = \Lambda_r - \lambda_r(t)M(t) - \mu_r M(t), \\ {}^{KKA}D_t^{\alpha}J(t) = \lambda_r(t)M(t) - \mu_r J(t), \end{cases} \tag{2.1}$$

with the following initial data:

$$S(0) = S_0 > 0,\ I(0) = I_0 \geq 0,\ R(0) = R_0 \geq 0,\ M(0) = M_0 > 0,\ J(0) = J_0 \geq 0. \tag{2.2}$$

System (2.1) has a clear epidemiological interpretation. The susceptible human class increases through recruitment and waning immunity, and decreases through infection and natural death. The infected human class grows through newly generated infections and declines because of recovery, natural mortality, and disease-related death. The recovered class is generated by successful recovery and is reduced by natural death and loss of immunity. On the rodent side, susceptible rodents are replenished by recruitment and diminished through infection and natural death, whereas infected rodents arise through transmission and leave the class through natural mortality.

For the analysis that follows, it is useful to represent the governing system in a vector setting. We set $X(t) = (S(t), I(t), R(t), M(t), J(t))^{\top}$ and $X_0 = (S_0, I_0, R_0, M_0, J_0)^{\top}$. Accordingly, equation system (2.1) may be written in the concise form

$${}^{KKA}D_t^{\alpha}X(t) = F(t, X(t)), \qquad X(0) = X_0, \tag{2.3}$$

where

$$F(t, X) = \begin{pmatrix} \Lambda_h + \gamma R - \lambda_h S - \mu_h S \\ \lambda_h S - (\varepsilon + \mu_h + \delta_h)I \\ \varepsilon I - (\mu_h + \gamma)R \\ \Lambda_r - \lambda_r M - \mu_r M \\ \lambda_r M - \mu_r J \end{pmatrix}.$$

Using the inverse relationship between the KKA fractional derivative and the corresponding fractional integral, the compact model (2.3) admits the following equivalent Volterra-type integral representation:

$$X(t) = X_0 + \frac{\alpha}{KA(\alpha)} \int_0^t F(\tau, X(\tau))\, d\tau + \frac{1-\alpha}{KA(\alpha)\Gamma(1-\alpha)} \int_0^t (t-\tau)^{-\alpha} F(\tau, X(\tau))\, d\tau. \tag{2.4}$$

The representation (2.4) will play a central role in the sequel, since it provides the foundation for establishing positivity, boundedness, existence, uniqueness, Ulam-Hyers stability, and the KKA Adams-Bashforth numerical approximation. Therefore, the proposed formulation extends the classical Lassa fever system to the KKA fractional setting while preserving the epidemiological meaning of each compartment and incorporating memory effects into the human-rodent transmission process.

3. Mathematical foundations

This section presents the mathematical preliminaries necessary for establishing the results of this study.

3.1. Definitions

In this subsection, we provide the fundamental definitions necessary for this framework.

Definition 3.1. *Let f be a continuous function such that $f \in \mathbb{H}^1(a,b)$, $a < b \in \mathbb{R}$, and $\alpha \in \ ]0,1]$. Following [15], the KKA derivative in the Caputo sense is defined as*

$$ {}_{a}^{KKA}D_t^{\alpha} f(t) = \frac{KA(\alpha)}{1-\alpha} \int_a^t f'(\tau)\, e_{\alpha,\alpha}\Big(-\frac{\alpha}{1-\alpha}(t-\tau)\Big)\, d\tau, $$

where $\mathbb{H}^1$ denotes the Sobolev space, $KA(\alpha)$ is the normalization function with $KA(0) = KA(1) = 1$, and $e_{\alpha,\alpha}$ is the α-generalized exponential function

$$ e_{\alpha,\alpha}\Big(-\frac{\alpha}{1-\alpha}t\Big) = \sum_{j=0}^{\infty} \frac{\Big(-\frac{\alpha}{1-\alpha}\Big)^j}{\Gamma(\alpha j+\alpha)}\, t^{\alpha j+\alpha-1}. $$

Definition 3.2. *Let f be a continuous function such that $f \in \mathbb{H}^1(a,b)$, where $a < b \in \mathbb{R}$, and let $\alpha \in (0,1]$. Following [15], the KKA fractional integral is defined as*

$$ {}_{a}^{KKA}I_t^{\alpha} f(t) = \frac{\alpha}{KA(\alpha)} \int_a^t f(\tau)\, d\tau + \frac{1-\alpha}{KA(\alpha)\Gamma(1-\alpha)} \int_a^t f(\tau)(t-\tau)^{-\alpha}\, d\tau, $$

where $KA(\alpha)$ is the normalization function satisfying:

$$ KA(0) = KA(1) = 1 \quad \text{and} \quad KA(\alpha) = 1 - \alpha + \frac{\alpha}{\Gamma(\alpha)}. $$

3.2. Existence and boundedness of solutions

In this part, we establish the existence of solutions for the KKA fractional Lassa fever model on a finite time interval and verify that each solution remains inside a bounded region that is biologically meaningful.

Let $X(t) = (S(t), I(t), R(t), M(t), J(t))^\top$ and $X_0 = (S_0, I_0, R_0, M_0, J_0)^\top$, and recall the equivalent Volterra-type integral formulation

$$ X(t) = X_0 + \frac{\alpha}{KA(\alpha)} \int_0^t F(\tau, X(\tau))\, d\tau + \frac{1-\alpha}{KA(\alpha)\Gamma(1-\alpha)} \int_0^t (t-\tau)^{-\alpha} F(\tau, X(\tau))\, d\tau. \tag{3.1} $$

Theorem 3.1. *Let the initial data be such that $S_0 > 0, I_0 \geq 0, R_0 \geq 0, M_0 > 0$, and $J_0 \geq 0$. Therefore, on every finite interval $[0,T]$ with $T > 0$, Eq (2.1) admits at least one nonnegative continuous solution, namely, $X \in C([0,T], \mathbb{R}_+^5)$. Moreover, every solution remains bounded on $[0,T]$. More precisely, $N_h(t) \leq K_h, N_r(t) \leq K_r, t \in [0,T]$, where $N_h(t) = S(t) + I(t) + R(t), N_r(t) = M(t) + J(t)$, and*

$$ K_h = \max\left\{N_h(0), \frac{\Lambda_h}{\mu_h}\right\},\ K_r = \max\left\{N_r(0), \frac{\Lambda_r}{\mu_r}\right\}. $$

Consequently, the set $\Omega = \left\{(S, I, R, M, J) \in \mathbb{R}_+^5 : 0 \leq N_h \leq K_h,\ 0 \leq N_r \leq K_r\right\}$ *forms a bounded positively invariant set for the system.*

Proof. We divide the proof into two steps.

Step 1: Let $N_h(t) = S(t) + I(t) + R(t)$ and $N_r(t) = M(t) + J(t)$. By adding the first three equations in (2.1), we obtain

$$^{KKA}D_t^{\alpha} N_h(t) = {}^{KKA}D_t^{\alpha} S(t) + {}^{KKA}D_t^{\alpha} I(t) + {}^{KKA}D_t^{\alpha} R(t).$$

Using the model equations, this gives

$$^{KKA}D_t^{\alpha} N_h(t) = \Lambda_h + \gamma R - \lambda_h S - \mu_h S + \lambda_h S - (\varepsilon + \mu_h + \delta_h) I + \varepsilon I - (\mu_h + \gamma) R.$$

After simplification,

$$^{KKA}D_t^{\alpha} N_h(t) = \Lambda_h - \mu_h(S + I + R) - \delta_h I = \Lambda_h - \mu_h N_h(t) - \delta_h I(t) \leq \Lambda_h - \mu_h N_h(t),$$

since $I(t) \geq 0$.

Similarly, adding the last two equations of (2.1), we get

$$^{KKA}D_t^{\alpha} N_r(t) = {}^{KKA}D_t^{\alpha} M(t) + {}^{KKA}D_t^{\alpha} J(t) = \Lambda_r - \mu_r(M + J) = \Lambda_r - \mu_r N_r(t).$$

Hence,

$$^{KKA}D_t^{\alpha} N_h(t) \leq \Lambda_h - \mu_h N_h(t), \qquad {}^{KKA}D_t^{\alpha} N_r(t) \leq \Lambda_r - \mu_r N_r(t).$$

By the comparison principle for Caputo-type KKA fractional differential inequalities, it follows that

$$N_h(t) \leq \max\left\{N_h(0), \frac{\Lambda_h}{\mu_h}\right\} = K_h, \qquad N_r(t) \leq \max\left\{N_r(0), \frac{\Lambda_r}{\mu_r}\right\} = K_r.$$

Therefore, every solution is bounded on $[0, T]$, and the region Ω is bounded and positively invariant.

Step 2: For the fixed-point argument, we work in the Banach space $\mathcal{X} = C([0, T], \mathbb{R}^5)$, endowed with the supremum norm $\|X\|_\infty = \sup_{t\in[0,T]} \|X(t)\|$. Next, we introduce the mapping $\mathcal{T} : \mathcal{X} \to \mathcal{X}$ through

$$(\mathcal{T}X)(t) = X_0 + \frac{\alpha}{KA(\alpha)} \int_0^t F(\tau, X(\tau))\, d\tau + \frac{1-\alpha}{KA(\alpha)\Gamma(1-\alpha)} \int_0^t (t-\tau)^{-\alpha} F(\tau, X(\tau))\, d\tau. \tag{3.2}$$

Accordingly, the integral equation (3.1) can be treated as a fixed-point problem for the operator $\mathcal{T}$.

Since the solution remains in the bounded invariant set Ω, the vector field F is continuous on the compact set $[0, T] \times \Omega$. Hence, there exists a constant $M > 0$ such that $\|F(t, X)\| \leq M, \forall (t, X) \in [0, T] \times \Omega$. We have

$$\|(\mathcal{T}X)(t) - X_0\| \leq \frac{\alpha}{KA(\alpha)} \int_0^t \|F(\tau, X(\tau))\|\, d\tau + \frac{1-\alpha}{KA(\alpha)\Gamma(1-\alpha)} \int_0^t (t-\tau)^{-\alpha} \|F(\tau, X(\tau))\|\, d\tau.$$

Using the bound $\|F(\tau, X(\tau))\| \leq M$, we get

$$\|(\mathcal{T}X)(t) - X_0\| \leq \frac{\alpha M}{KA(\alpha)} \int_0^t d\tau + \frac{(1-\alpha)M}{KA(\alpha)\Gamma(1-\alpha)} \int_0^t (t-\tau)^{-\alpha}\, d\tau.$$

Since

$$\int_0^t d\tau = t, \qquad \int_0^t (t-\tau)^{-\alpha}\, d\tau = \frac{t^{1-\alpha}}{1-\alpha} = \frac{\Gamma(1-\alpha)}{\Gamma(2-\alpha)}\, t^{1-\alpha},$$

and it follows that

$$\|(\mathcal{T}X)(t) - X_0\| \leq M\left(\frac{\alpha t}{KA(\alpha)} + \frac{(1-\alpha)t^{1-\alpha}}{KA(\alpha)\Gamma(2-\alpha)}\right).$$

Hence,

$$\|(\mathcal{T}X) - X_0\|_\infty \leq M\left(\frac{\alpha T}{KA(\alpha)} + \frac{(1-\alpha)T^{1-\alpha}}{KA(\alpha)\Gamma(2-\alpha)}\right).$$

We therefore conclude that $\mathcal{T}$ maps bounded sets into bounded sets. Furthermore, the usual estimates for weakly singular Volterra integral operators ensure that $\mathcal{T}$ also sends bounded sets into equicontinuous families. By applying the Arzelà–Ascoli theorem, one deduces that $\mathcal{T}$ is compact.

Since the set Ω is nonempty and has the properties of being closed, bounded, and convex, Schauder's fixed-point theorem can be applied to infer that $\mathcal{T}$ has a fixed point in $\mathcal{X}$. Therefore, model (2.1) has at least one solution on $[0, T]$.

The conclusion follows by combining the two steps above. □

3.3. *Invertibility of the KKA operators and the integral form of the model*

The analysis of the proposed Lassa fever system relies heavily on the inverse property between the KKA fractional differential operator and the corresponding integral operator. By exploiting this relation, the governing equations can be converted into a Volterra-type integral form, providing a more suitable setting for the study of solvability, stability, and numerical approximation.

Theorem 3.2. *Let $f \in H^1(0, T)$ and $0 < \alpha \leq 1$. Then the KKA fractional derivative in the Caputo sense and the KKA fractional integral satisfy the following invertibility relations:*

$$ {}_0^{KKA}I_t^\alpha\left({}_0^{KKA}D_t^\alpha f(t)\right) = f(t) - f(0) \tag{3.3}$$

and

$$ {}_0^{KKA}D_t^\alpha\left({}_0^{KKA}I_t^\alpha f(t)\right) = f(t). \tag{3.4}$$

Proof. Let $F(p) = \mathcal{L}\{f(t)\}(p)$. We prove the two identities separately by using the definitions of the KKA fractional derivative and KKA fractional integral together with the Laplace transform. Recall that

$$ {}_0^{KKA}I_t^\alpha f(t) = \frac{\alpha}{KA(\alpha)}\int_0^t f(\tau)\, d\tau + \frac{1-\alpha}{KA(\alpha)\Gamma(1-\alpha)}\int_0^t f(\tau)(t-\tau)^{-\alpha}\, d\tau \tag{3.5}$$

and

$$ {}_0^{KKA}D_t^\alpha f(t) = \frac{KA(\alpha)}{1-\alpha}\int_0^t f'(\tau)\, e_{\alpha,\alpha}\left(-\frac{\alpha}{1-\alpha}(t-\tau)\right) d\tau. \tag{3.6}$$

Since the KKA derivative is given in convolution form, we may write

$$ {}_0^{KKA}D_t^\alpha f(t) = \frac{KA(\alpha)}{1-\alpha}\left(f'(t) * e_{\alpha,\alpha}\left(-\tfrac{\alpha}{1-\alpha}t\right)\right).$$

Using the Laplace transform of the generalized exponential kernel,

$$\mathcal{L}\left\{e_{\alpha,\alpha}\left(-\frac{\alpha}{1-\alpha}t\right)\right\}(p) = \frac{1}{p^{\alpha} + \frac{\alpha}{1-\alpha}},$$

together with $\mathcal{L}\{f'(t)\}(p) = pF(p) - f(0)$, we obtain

$$\mathcal{L}\left\{{}_{0}^{KKA}D_{t}^{\alpha} f(t)\right\}(p) = \frac{KA(\alpha)}{1-\alpha}\frac{pF(p) - f(0)}{p^{\alpha} + \frac{\alpha}{1-\alpha}}. \tag{3.7}$$

Also, from (3.5),

$${}_{0}^{KKA}I_{t}^{\alpha} f(t) = \frac{\alpha}{KA(\alpha)}(f * 1)(t) + \frac{1-\alpha}{KA(\alpha)\Gamma(1-\alpha)}(f * t^{-\alpha})(t).$$

Hence, using

$$\mathcal{L}\{1\}(p) = \frac{1}{p}, \qquad \mathcal{L}\{t^{-\alpha}\}(p) = \Gamma(1-\alpha)\, p^{\alpha-1} = \frac{\Gamma(1-\alpha)}{p^{1-\alpha}},$$

we get

$$\mathcal{L}\left\{{}_{0}^{KKA}I_{t}^{\alpha} f(t)\right\}(p) = \frac{\alpha}{KA(\alpha)}\frac{F(p)}{p} + \frac{1-\alpha}{KA(\alpha)}\frac{F(p)}{p^{1-\alpha}}. \tag{3.8}$$

Set $k(t) = {}_{0}^{KKA}D_{t}^{\alpha} f(t)$. Then, by (3.8),

$$\mathcal{L}\left\{{}_{0}^{KKA}I_{t}^{\alpha}\left({}_{0}^{KKA}D_{t}^{\alpha} f(t)\right)\right\}(p) = \frac{\alpha}{KA(\alpha)}\frac{\mathcal{L}\{k(t)\}(p)}{p} + \frac{1-\alpha}{KA(\alpha)}\frac{\mathcal{L}\{k(t)\}(p)}{p^{1-\alpha}}.$$

Substituting (3.7) into the above relation yields

$$\begin{aligned}
\mathcal{L}\left\{{}_{0}^{KKA}I_{t}^{\alpha}\left({}_{0}^{KKA}D_{t}^{\alpha} f(t)\right)\right\}(p) &= \frac{\alpha}{KA(\alpha)}\frac{1}{p}\left(\frac{KA(\alpha)}{1-\alpha}\frac{pF(p) - f(0)}{p^{\alpha} + \frac{\alpha}{1-\alpha}}\right) + \frac{1-\alpha}{KA(\alpha)}\frac{1}{p^{1-\alpha}}\left(\frac{KA(\alpha)}{1-\alpha}\frac{pF(p) - f(0)}{p^{\alpha} + \frac{\alpha}{1-\alpha}}\right) \\
&= \frac{\alpha}{1-\alpha}\,\frac{pF(p) - f(0)}{p\left(p^{\alpha} + \frac{\alpha}{1-\alpha}\right)} + \frac{p^{\alpha-1}(pF(p) - f(0))}{p^{\alpha} + \frac{\alpha}{1-\alpha}}.
\end{aligned}$$

Factoring $\frac{pF(p) - f(0)}{p}$, we obtain

$$\begin{aligned}
\mathcal{L}\left\{{}_{0}^{KKA}I_{t}^{\alpha}\left({}_{0}^{KKA}D_{t}^{\alpha} f(t)\right)\right\}(p) &= \frac{pF(p) - f(0)}{p}\left(\frac{\frac{\alpha}{1-\alpha} + p^{\alpha}}{p^{\alpha} + \frac{\alpha}{1-\alpha}}\right) \\
&= \frac{pF(p) - f(0)}{p} \\
&= F(p) - \frac{f(0)}{p}.
\end{aligned}$$

Applying the inverse Laplace transform gives ${}_0^{KKA}I_t^{\alpha}\Big({}_0^{KKA}D_t^{\alpha}f(t)\Big) = f(t) - f(0)$. Now let $h(t) = {}_0^{KKA}I_t^{\alpha}f(t)$. Since the KKA integral starts from 0, we have $h(0) = {}_0^{KKA}I_0^{\alpha}f(0) = 0$. Using (3.7), we obtain

$$\mathcal{L}\Big\{{}_0^{KKA}D_t^{\alpha}h(t)\Big\}(p) = \frac{KA(\alpha)}{1-\alpha}\frac{p\,\mathcal{L}\{h(t)\}(p) - h(0)}{p^{\alpha} + \dfrac{\alpha}{1-\alpha}} = \frac{KA(\alpha)}{1-\alpha}\frac{p\,\mathcal{L}\{h(t)\}(p)}{p^{\alpha} + \dfrac{\alpha}{1-\alpha}}.$$

From (3.8), we have

$$\mathcal{L}\{h(t)\}(p) = \frac{\alpha}{KA(\alpha)}\frac{F(p)}{p} + \frac{1-\alpha}{KA(\alpha)}\frac{F(p)}{p^{1-\alpha}}.$$

Therefore,

$$\begin{aligned}\mathcal{L}\Big\{{}_0^{KKA}D_t^{\alpha}\Big({}_0^{KKA}I_t^{\alpha}f(t)\Big)\Big\}(p) &= \frac{KA(\alpha)}{1-\alpha}\frac{p}{p^{\alpha} + \dfrac{\alpha}{1-\alpha}}\left(\frac{\alpha}{KA(\alpha)}\frac{F(p)}{p} + \frac{1-\alpha}{KA(\alpha)}\frac{F(p)}{p^{1-\alpha}}\right)\\ &= \frac{\alpha}{1-\alpha}\frac{F(p)}{p^{\alpha} + \dfrac{\alpha}{1-\alpha}} + \frac{p^{\alpha}F(p)}{p^{\alpha} + \dfrac{\alpha}{1-\alpha}}\\ &= F(p).\end{aligned}$$

Taking the inverse Laplace transform, we conclude that ${}_0^{KKA}D_t^{\alpha}\Big({}_0^{KKA}I_t^{\alpha}f(t)\Big) = f(t)$. Hence, the KKA fractional derivative and the KKA fractional integral satisfy the invertibility relations (3.3) and (3.4). This completes the proof. □

We now apply Theorem 3.2 to the KKA fractional-order Lassa fever model

$$\begin{cases} {}_0^{KKA}D_t^{\alpha}S(t) = \Lambda_h + \gamma R(t) - \lambda_h(t)S(t) - \mu_h S(t),\\ {}_0^{KKA}D_t^{\alpha}I(t) = \lambda_h(t)S(t) - (\varepsilon + \mu_h + \delta_h)I(t),\\ {}_0^{KKA}D_t^{\alpha}R(t) = \varepsilon I(t) - (\mu_h + \gamma)R(t),\\ {}_0^{KKA}D_t^{\alpha}M(t) = \Lambda_r - \lambda_r(t)M(t) - \mu_r M(t),\\ {}_0^{KKA}D_t^{\alpha}J(t) = \lambda_r(t)M(t) - \mu_r J(t), \end{cases} \tag{3.9}$$

where $\lambda_h(t) = \frac{\beta_h I(t) + \beta_r J(t)}{N_h(t)}$ and $\lambda_r(t) = \frac{\beta_{hr} I(t)}{N_r(t)}$, with $N_h(t) = S(t) + I(t) + R(t)$ and $N_r(t) = M(t) + J(t)$. Applying the operator ${}_0^{KKA}I_t^{\alpha}$ to each equation of (3.9) and using (3.3), we obtain the equivalent integral representation

$$\begin{aligned} S(t) = S_0 &+ \frac{\alpha}{KA(\alpha)}\int_0^t \Big[\Lambda_h + \gamma R(\tau) - \lambda_h(\tau)S(\tau) - \mu_h S(\tau)\Big]d\tau\\ &+ \frac{1-\alpha}{KA(\alpha)\Gamma(1-\alpha)}\int_0^t (t-\tau)^{-\alpha}\Big[\Lambda_h + \gamma R(\tau) - \lambda_h(\tau)S(\tau) - \mu_h S(\tau)\Big]d\tau, \end{aligned} \tag{3.10}$$

$$\begin{aligned} I(t) = I_0 &+ \frac{\alpha}{KA(\alpha)}\int_0^t \Big[\lambda_h(\tau)S(\tau) - (\varepsilon + \mu_h + \delta_h)I(\tau)\Big]d\tau\\ &+ \frac{1-\alpha}{KA(\alpha)\Gamma(1-\alpha)}\int_0^t (t-\tau)^{-\alpha}\Big[\lambda_h(\tau)S(\tau) - (\varepsilon + \mu_h + \delta_h)I(\tau)\Big]d\tau, \end{aligned} \tag{3.11}$$

$$
\begin{aligned}
R(t) = R_0 + \frac{\alpha}{KA(\alpha)} \int_0^t \Big[\varepsilon I(\tau) - (\mu_h + \gamma) R(\tau)\Big]\, d\tau \\
+ \frac{1-\alpha}{KA(\alpha)\Gamma(1-\alpha)} \int_0^t (t-\tau)^{-\alpha} \Big[\varepsilon I(\tau) - (\mu_h + \gamma) R(\tau)\Big]\, d\tau,
\end{aligned}
\tag{3.12}
$$

$$
\begin{aligned}
M(t) = M_0 + \frac{\alpha}{KA(\alpha)} \int_0^t \Big[\Lambda_r - \lambda_r(\tau) M(\tau) - \mu_r M(\tau)\Big]\, d\tau \\
+ \frac{1-\alpha}{KA(\alpha)\Gamma(1-\alpha)} \int_0^t (t-\tau)^{-\alpha} \Big[\Lambda_r - \lambda_r(\tau) M(\tau) - \mu_r M(\tau)\Big]\, d\tau,
\end{aligned}
\tag{3.13}
$$

$$
\begin{aligned}
J(t) = J_0 + \frac{\alpha}{KA(\alpha)} \int_0^t \Big[\lambda_r(\tau) M(\tau) - \mu_r J(\tau)\Big]\, d\tau \\
+ \frac{1-\alpha}{KA(\alpha)\Gamma(1-\alpha)} \int_0^t (t-\tau)^{-\alpha} \Big[\lambda_r(\tau) M(\tau) - \mu_r J(\tau)\Big]\, d\tau.
\end{aligned}
\tag{3.14}
$$

We introduce the notation $X(t) = (S(t), I(t), R(t), M(t), J(t))^\top$ and $X_0 = (S_0, I_0, R_0, M_0, J_0)^\top$. Hence, Eqs (3.10)–(3.14) admit the following compact representation:

$$
X(t) = X_0 + \frac{\alpha}{KA(\alpha)} \int_0^t F(\tau, X(\tau))\, d\tau + \frac{1-\alpha}{KA(\alpha)\Gamma(1-\alpha)} \int_0^t (t-\tau)^{-\alpha} F(\tau, X(\tau))\, d\tau, \tag{3.15}
$$

where

$$
F(t, X) = \begin{pmatrix}
\Lambda_h + \gamma R - \lambda_h S - \mu_h S \\
\lambda_h S - (\varepsilon + \mu_h + \delta_h) I \\
\varepsilon I - (\mu_h + \gamma) R \\
\Lambda_r - \lambda_r M - \mu_r M \\
\lambda_r M - \mu_r J
\end{pmatrix}.
$$

The representation (3.15) is equivalent to the original KKA fractional differential system and will be used throughout the rest of the paper. In particular, it provides the basic framework for the uniqueness proof presented in the next subsection, as well as for Ulam-Hyers stability and the construction of the KKA Adams-Bashforth numerical scheme.

3.4. Uniqueness of the solution

We now establish the uniqueness of the solution of the proposed KKA fractional-order Lassa fever model. Let $X(t) = (S(t), I(t), R(t), M(t), J(t))^\top$ and consider the equivalent Volterra-type integral representation

$$
X(t) = X_0 + \frac{\alpha}{KA(\alpha)} \int_0^t F(\tau, X(\tau)) d\tau + \frac{1-\alpha}{KA(\alpha)\Gamma(1-\alpha)} \int_0^t (t-\tau)^{-\alpha} F(\tau, X(\tau)) d\tau.
$$

Let Ω be the bounded positively invariant region obtained in Theorem 3.1. Since the right-hand side $F(t, X)$ is continuously differentiable with respect to X on the bounded set $[0, T] \times \Omega$, it is locally Lipschitz continuous in X. Hence, there exists a constant $L > 0$ such that

$$
\|F(t, X) - F(t, Y)\| \le L \|X - Y\|, \ t \in [0, T], \ X, Y \in \Omega.
$$

Define the operator $\mathcal{T} : C([0, T], \mathbb{R}^5) \to C([0, T], \mathbb{R}^5)$ by

$$(\mathcal{T}X)(t) = X_0 + \frac{\alpha}{KA(\alpha)} \int_0^t F(\tau, X(\tau))d\tau + \frac{1-\alpha}{KA(\alpha)\Gamma(1-\alpha)} \int_0^t (t-\tau)^{-\alpha} F(\tau, X(\tau))d\tau.$$

For any $X, Y \in C([0, T], \mathbb{R}^5)$, we obtain

$$\begin{aligned}\|(\mathcal{T}X)(t) - (\mathcal{T}Y)(t)\| \le{}& \frac{\alpha}{KA(\alpha)} \int_0^t \|F(\tau, X(\tau)) - F(\tau, Y(\tau))\|d\tau \\ &+ \frac{1-\alpha}{KA(\alpha)\Gamma(1-\alpha)} \int_0^t (t-\tau)^{-\alpha} \|F(\tau, X(\tau)) - F(\tau, Y(\tau))\|d\tau.\end{aligned}$$

Using the Lipschitz condition, we have

$$\|(\mathcal{T}X)(t) - (\mathcal{T}Y)(t)\| \le L\|X - Y\|_\infty \left[\frac{\alpha t}{KA(\alpha)} + \frac{(1-\alpha)t^{1-\alpha}}{KA(\alpha)\Gamma(2-\alpha)}\right].$$

Taking the supremum over $t \in [0, T]$, it follows that $\|\mathcal{T}X - \mathcal{T}Y\|_\infty \le LQ_T\|X - Y\|_\infty$, where

$$Q_T = \frac{\alpha T}{KA(\alpha)} + \frac{(1-\alpha)T^{1-\alpha}}{KA(\alpha)\Gamma(2-\alpha)}.$$

If $LQ_T < 1$, then $\mathcal{T}$ is a contraction on $C([0, T], \mathbb{R}^5)$. Therefore, by the Banach fixed-point theorem, the operator $\mathcal{T}$ has a unique fixed point. Consequently, the integral equation and hence the original KKA fractional-order Lassa fever model possess a unique solution on $[0, T]$.

For a general finite interval, the same argument can be applied successively on sufficiently small subintervals, where the contraction condition is satisfied. Therefore, the solution of the proposed model is unique on every finite interval. This completes the proof of uniqueness.

4. KKA Adams-Bashforth numerical scheme

In this section, we construct a two-step Adams-Bashforth-type numerical method for the KKA fractional-order Lassa fever model. The proposed discretization is derived from the equivalent Volterra-type integral formulation established in the previous section and is then written explicitly for all state variables of the system.

Let $X(t) = (S(t), I(t), R(t), M(t), J(t))^\top$ and $X_0 = (S_0, I_0, R_0, M_0, J_0)^\top$, and consider the compact form

$${}_0^{KKA}D_t^\alpha X(t) = F(t, X(t)), \qquad 0 < \alpha \le 1, \tag{4.1}$$

where

$$F(t, X) = \begin{pmatrix} F_S(t, X) \\ F_I(t, X) \\ F_R(t, X) \\ F_M(t, X) \\ F_J(t, X) \end{pmatrix},$$

with

$$F_S(t, X) = \Lambda_h + \gamma R - \lambda_h S - \mu_h S,$$

$$
\begin{aligned}
F_I(t,X) &= \lambda_h S - (\varepsilon + \mu_h + \delta_h) I,\\
F_R(t,X) &= \varepsilon I - (\mu_h + \gamma) R,\\
F_M(t,X) &= \Lambda_r - \lambda_r M - \mu_r M,\\
F_J(t,X) &= \lambda_r M - \mu_r J,
\end{aligned}
$$

and

$$
\lambda_h = \frac{\beta_h I + \beta_r J}{S + I + R},\ \lambda_r = \frac{\beta_{hr} I}{M + J}.
$$

By the invertibility relation of the KKA operators, system (4.1) is

$$
X(t) = X_0 + \frac{\alpha}{KA(\alpha)} \int_0^t F(\tau, X(\tau))\, d\tau + \frac{1-\alpha}{KA(\alpha)\Gamma(1-\alpha)} \int_0^t (t-\tau)^{-\alpha} F(\tau, X(\tau))\, d\tau. \tag{4.2}
$$

Let $t_n = nh$, where $h > 0$ is the time step, and let $X_n \approx X(t_n)$. We also denote $F_n = F(t_n, X_n)$. Evaluating (4.2) at $t = t_{n+1}$ and $t = t_n$, and then subtracting the resulting expressions, we obtain

$$
\begin{aligned}
X(t_{n+1}) - X(t_n) &= \frac{\alpha}{KA(\alpha)} \int_{t_n}^{t_{n+1}} F(\tau, X(\tau))\, d\tau\\
&+ \frac{1-\alpha}{KA(\alpha)\Gamma(1-\alpha)} \left[\int_0^{t_{n+1}} (t_{n+1}-\tau)^{-\alpha} F(\tau, X(\tau))\, d\tau - \int_0^{t_n} (t_n-\tau)^{-\alpha} F(\tau, X(\tau))\, d\tau \right].
\end{aligned} \tag{4.3}
$$

To derive a two-step Adams-Bashforth approximation, we interpolate $F(\tau, X(\tau))$ on $[t_{n-1}, t_n]$ by the linear Lagrange polynomial

$$
F(\tau, X(\tau)) \approx \frac{\tau - t_{n-1}}{h} F_n - \frac{\tau - t_n}{h} F_{n-1}. \tag{4.4}
$$

After substituting (4.4) into (4.3) and performing the necessary integrations, the recurrence relation takes the form of (4.5).

Proposition 4.1. *For $n \geq 1$, the two-step KKA Adams-Bashforth approximation of* (4.1) *is given by*

$$
X_{n+1} = X_n + \frac{\alpha h}{2KA(\alpha)} (3F_n - F_{n-1}) + \frac{1-\alpha}{h\, KA(\alpha)\Gamma(2-\alpha)} \Big(\omega_{n+1} F_n - \eta_{n+1} F_{n-1} \Big), \tag{4.5}
$$

where

$$
\omega_{n+1} = 2h\, t_{n+1}^{1-\alpha} - h\, t_n^{1-\alpha} - \frac{1-\alpha}{2-\alpha} \Big(t_{n+1}^{2-\alpha} - t_n^{2-\alpha} \Big) \tag{4.6}
$$

and

$$
\eta_{n+1} = h\, t_{n+1}^{1-\alpha} - \frac{1-\alpha}{2-\alpha} \Big(t_{n+1}^{2-\alpha} - t_n^{2-\alpha} \Big). \tag{4.7}
$$

Proof. Using the interpolation formula (4.4), the first integral in (4.3) becomes

$$
\int_{t_n}^{t_{n+1}} F(\tau, X(\tau))\, d\tau \approx \int_{t_n}^{t_{n+1}} \left(\frac{\tau - t_{n-1}}{h} F_n - \frac{\tau - t_n}{h} F_{n-1} \right) d\tau = \frac{h}{2} (3F_n - F_{n-1}).
$$

Similarly, substituting (4.4) into the memory contribution in (4.3) and integrating term-by-term yields

$$
\int_0^{t_{n+1}} (t_{n+1}-\tau)^{-\alpha} F(\tau, X(\tau))\, d\tau - \int_0^{t_n} (t_n-\tau)^{-\alpha} F(\tau, X(\tau))\, d\tau \approx \frac{1}{h} \Big(\omega_{n+1} F_n - \eta_{n+1} F_{n-1} \Big),
$$

where ω_{n+1} and η_{n+1} are given by (4.6) and (4.7). Substituting these approximations into (4.3) completes the derivation of (4.5). □

For implementation, we write (4.5) componentwise. Let

$$\lambda_{h,n} = \frac{\beta_h I_n + \beta_r J_n}{S_n + I_n + R_n}, \lambda_{r,n} = \frac{\beta_{hr} I_n}{M_n + J_n},$$

and define

$$\begin{aligned}
F_{S,n} &= \Lambda_h + \gamma R_n - \lambda_{h,n} S_n - \mu_h S_n, \\
F_{I,n} &= \lambda_{h,n} S_n - (\varepsilon + \mu_h + \delta_h) I_n, \\
F_{R,n} &= \varepsilon I_n - (\mu_h + \gamma) R_n, \\
F_{M,n} &= \Lambda_r - \lambda_{r,n} M_n - \mu_r M_n, \\
F_{J,n} &= \lambda_{r,n} M_n - \mu_r J_n.
\end{aligned}$$

Then the numerical updates read

$$\begin{aligned}
S_{n+1} &= S_n + \frac{\alpha h}{2KA(\alpha)}(3F_{S,n} - F_{S,n-1}) + \frac{1-\alpha}{h\,KA(\alpha)\Gamma(2-\alpha)}\Big(\omega_{n+1} F_{S,n} - \eta_{n+1} F_{S,n-1}\Big), \\
I_{n+1} &= I_n + \frac{\alpha h}{2KA(\alpha)}(3F_{I,n} - F_{I,n-1}) + \frac{1-\alpha}{h\,KA(\alpha)\Gamma(2-\alpha)}\Big(\omega_{n+1} F_{I,n} - \eta_{n+1} F_{I,n-1}\Big), \\
R_{n+1} &= R_n + \frac{\alpha h}{2KA(\alpha)}(3F_{R,n} - F_{R,n-1}) + \frac{1-\alpha}{h\,KA(\alpha)\Gamma(2-\alpha)}\Big(\omega_{n+1} F_{R,n} - \eta_{n+1} F_{R,n-1}\Big), \\
M_{n+1} &= M_n + \frac{\alpha h}{2KA(\alpha)}(3F_{M,n} - F_{M,n-1}) + \frac{1-\alpha}{h\,KA(\alpha)\Gamma(2-\alpha)}\Big(\omega_{n+1} F_{M,n} - \eta_{n+1} F_{M,n-1}\Big), \\
J_{n+1} &= J_n + \frac{\alpha h}{2KA(\alpha)}(3F_{J,n} - F_{J,n-1}) + \frac{1-\alpha}{h\,KA(\alpha)\Gamma(2-\alpha)}\Big(\omega_{n+1} F_{J,n} - \eta_{n+1} F_{J,n-1}\Big).
\end{aligned} \tag{4.8}$$

Since (4.5) is a two-step scheme, one additional starting value is required. We compute X_1 from a one-step KKA Euler-type approximation:

$$X_1 = X_0 + \frac{\alpha h}{KA(\alpha)} F_0 + \frac{(1-\alpha)h^{1-\alpha}}{KA(\alpha)\Gamma(2-\alpha)} F_0. \tag{4.9}$$

Equivalently, the starting values for the five compartments are

$$\begin{aligned}
S_1 &= S_0 + \frac{\alpha h}{KA(\alpha)} F_{S,0} + \frac{(1-\alpha)h^{1-\alpha}}{KA(\alpha)\Gamma(2-\alpha)} F_{S,0}, \\
I_1 &= I_0 + \frac{\alpha h}{KA(\alpha)} F_{I,0} + \frac{(1-\alpha)h^{1-\alpha}}{KA(\alpha)\Gamma(2-\alpha)} F_{I,0}, \\
R_1 &= R_0 + \frac{\alpha h}{KA(\alpha)} F_{R,0} + \frac{(1-\alpha)h^{1-\alpha}}{KA(\alpha)\Gamma(2-\alpha)} F_{R,0}, \\
M_1 &= M_0 + \frac{\alpha h}{KA(\alpha)} F_{M,0} + \frac{(1-\alpha)h^{1-\alpha}}{KA(\alpha)\Gamma(2-\alpha)} F_{M,0}, \\
J_1 &= J_0 + \frac{\alpha h}{KA(\alpha)} F_{J,0} + \frac{(1-\alpha)h^{1-\alpha}}{KA(\alpha)\Gamma(2-\alpha)} F_{J,0}.
\end{aligned}$$

If $F \in C^2$ over the interval of integration, then the scheme has the following local truncation error:

$$\mathcal{R}_{n+1} = O(h^3) + O(h^{3-\alpha}), \qquad 0 < \alpha \leq 1, \tag{4.10}$$

which shows that the proposed KKA Adams-Bashforth method is consistent. Therefore, schemes (4.5)–(4.8) provide an effective numerical procedure for simulating the fractional-order Lassa fever model for different values of the derivative order α.

For all simulations reported in this paper, the numerical trajectories are generated by initializing the method with (4.9) and then iterating the recurrence relation (4.8) over the prescribed time interval.

5. Numerical simulations and discussion

In this section, we apply the KKA Adams-Bashforth scheme developed in Section 4 to simulate the fractional Lassa fever system. The purpose is to examine how memory influences the transmission process by considering different values of $0 < \alpha \leq 1$, while all remaining parameters are fixed as listed in Table 1. The baseline parameter values used in the numerical simulations are reported in Table 1. Parameters available from previous Lassa fever modeling studies are cited accordingly, while the remaining parameters are fixed for numerical illustration when direct data are not available. These assumed values are selected within biologically meaningful ranges in order to demonstrate the qualitative behavior of the proposed KKA fractional-order model. Unless otherwise stated, all simulations are performed using the same baseline parameter set, and one parameter is varied at a time when studying parameter effects.

Table 1. Parameter values, sources, and sensitivity indices.

Parameter	Parameter value	Source	Sensitivity index
Λ_h	10	[7]	–
γ	0.0150	Assumed	–
ϵ	0.1000	Assumed	-0.0767240
μ_h	0.0003	[1]	-0.0002302
δ_h	0.6	Assumed	-0.4603440
α_h	0.0100	Assumed	+0.07459680
α_r	0.0200	Assumed	+0.9254030
Λ_r	0.1000	[1]	–
μ_r	0.0627	[1]	-0.4627020

For clarity and reproducibility, the initial conditions used in the simulations are $S(0) = 700$, $I(0) = 120$, $R(0) = 30$, $M(0) = 250$, and $J(0) = 60$. The simulations are carried out on the time interval $0 \leq t \leq 20$ with time step $h = 0.02$. The fractional orders considered are $\alpha = 1.00, 0.80, 0.40$, and 0.10, where $\alpha = 1$ represents the classical integer-order case and $0 < \alpha < 1$ represents the memory-dependent fractional case. To simplify the notation, the right-hand side of the governing system is represented as

$${}_0^{KKA}D_t^\alpha S(t) = \Phi_1(t), {}_0^{KKA}D_t^\alpha I(t) = \Phi_2(t), {}_0^{KKA}D_t^\alpha R(t) = \Phi_3(t), {}_0^{KKA}D_t^\alpha M(t) = \Phi_4(t), {}_0^{KKA}D_t^\alpha J(t) = \Phi_5(t),$$

where

$$\begin{aligned}
\Phi_1(t) &= \Lambda_h + \gamma R(t) - \lambda_h(t)S(t) - \mu_h S(t),\\
\Phi_2(t) &= \lambda_h(t)S(t) - (\varepsilon + \mu_h + \delta_h)I(t),\\
\Phi_3(t) &= \varepsilon I(t) - (\mu_h + \gamma)R(t),\\
\Phi_4(t) &= \Lambda_r - \lambda_r(t)M(t) - \mu_r M(t),\\
\Phi_5(t) &= \lambda_r(t)M(t) - \mu_r J(t),
\end{aligned}$$

with

$$\lambda_h(t) = \frac{\beta_h I(t) + \beta_r J(t)}{S(t) + I(t) + R(t)},$$

$$\lambda_r(t) = \frac{\beta_{hr} I(t)}{M(t) + J(t)}.$$

Accordingly, the numerical approximations satisfy

$$S_{n+1} = S_n + \frac{\alpha h}{2KA(\alpha)}(3\Phi_{1,n} - \Phi_{1,n-1}) + \frac{1-\alpha}{h\,KA(\alpha)\Gamma(2-\alpha)}(\omega_{n+1}\Phi_{1,n} - \eta_{n+1}\Phi_{1,n-1}),$$

$$I_{n+1} = I_n + \frac{\alpha h}{2KA(\alpha)}(3\Phi_{2,n} - \Phi_{2,n-1}) + \frac{1-\alpha}{h\,KA(\alpha)\Gamma(2-\alpha)}(\omega_{n+1}\Phi_{2,n} - \eta_{n+1}\Phi_{2,n-1}),$$

$$R_{n+1} = R_n + \frac{\alpha h}{2KA(\alpha)}(3\Phi_{3,n} - \Phi_{3,n-1}) + \frac{1-\alpha}{h\,KA(\alpha)\Gamma(2-\alpha)}(\omega_{n+1}\Phi_{3,n} - \eta_{n+1}\Phi_{3,n-1}),$$

$$M_{n+1} = M_n + \frac{\alpha h}{2KA(\alpha)}(3\Phi_{4,n} - \Phi_{4,n-1}) + \frac{1-\alpha}{h\,KA(\alpha)\Gamma(2-\alpha)}(\omega_{n+1}\Phi_{4,n} - \eta_{n+1}\Phi_{4,n-1}),$$

$$J_{n+1} = J_n + \frac{\alpha h}{2KA(\alpha)}(3\Phi_{5,n} - \Phi_{5,n-1}) + \frac{1-\alpha}{h\,KA(\alpha)\Gamma(2-\alpha)}(\omega_{n+1}\Phi_{5,n} - \eta_{n+1}\Phi_{5,n-1}),$$

where

$$\omega_{n+1} = 2h\,t_{n+1}^{1-\alpha} - h\,t_n^{1-\alpha} - \frac{1-\alpha}{2-\alpha}\Big(t_{n+1}^{2-\alpha} - t_n^{2-\alpha}\Big)$$

and

$$\eta_{n+1} = h\,t_{n+1}^{1-\alpha} - \frac{1-\alpha}{2-\alpha}\Big(t_{n+1}^{2-\alpha} - t_n^{2-\alpha}\Big).$$

The numerical simulations are performed over the interval $0 \le t \le T$ with time step h, and the resulting numerical trajectories are displayed in Figures 1–3. Figure 1 presents the temporal evolution of the susceptible, infected, and recovered human populations together with the susceptible and infected rodent populations for different values of the fractional order α, as well as the corresponding two-dimensional phase trajectory in the $(I(t), J(t))$ plane. Figure 2 shows the two-dimensional phase portraits in the $(S(t), I(t))$, $(M(t), J(t))$, and $(S(t), R(t))$ planes, while Figure 3 displays the three-dimensional phase portraits in the $(S(t), I(t), R(t))$, $(M(t), I(t), J(t))$, and $(M(t), S(t), J(t))$ spaces. These figures provide both temporal and geometric descriptions of the influence of memory on the interaction among the epidemiological compartments.

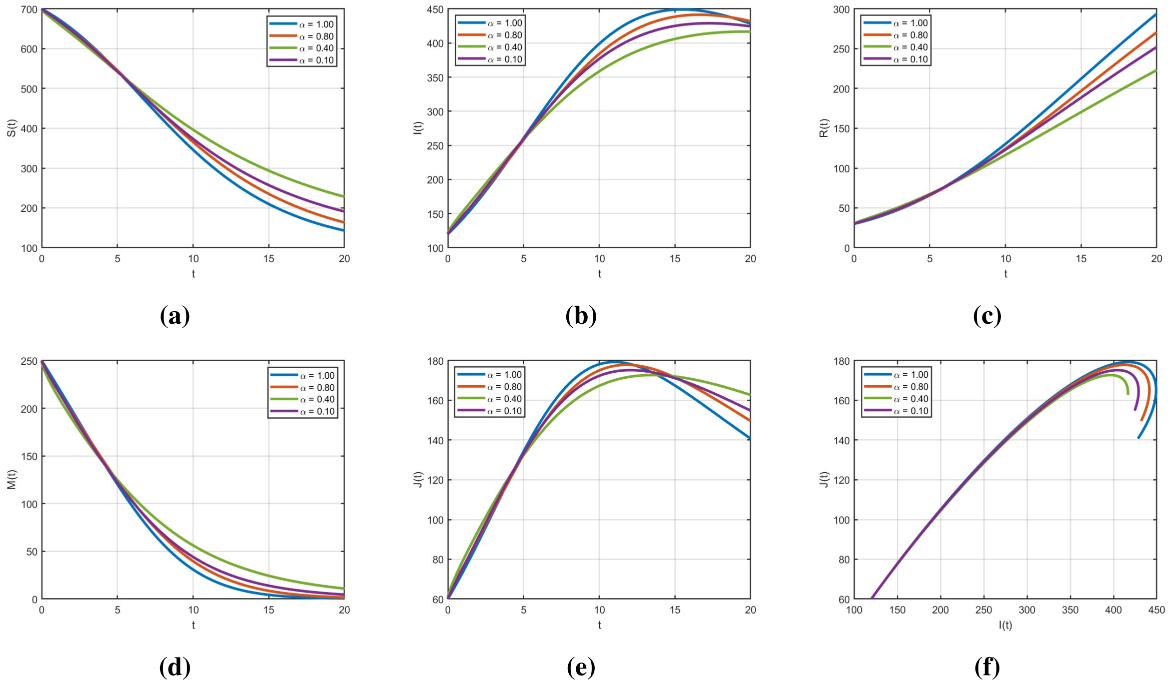

Figure 1. Time profiles and phase portrait of the KKA fractional-order Lassa fever model for selected values of the fractional order α. The panels show the temporal evolution of $S(t)$, $I(t)$, $R(t)$, $M(t)$, and $J(t)$, together with the two-dimensional phase trajectory in the $(I(t), J(t))$ plane. The numerical results indicate that $S(t)$ and $M(t)$ decrease over time, $R(t)$ increases, while $I(t)$ and $J(t)$ initially rise to peak levels and then decline. Moreover, smaller values of α produce smoother trajectories and slower epidemic progression, reflecting stronger memory effects in both the human and rodent populations.

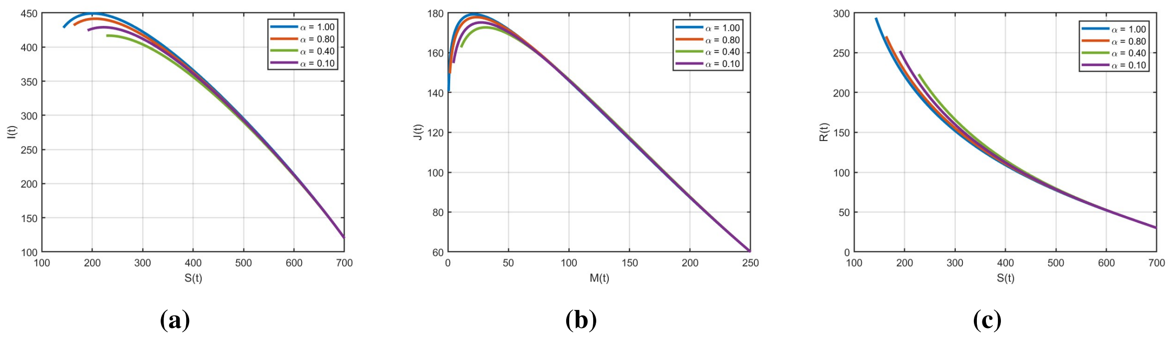

Figure 2. Two-dimensional phase portraits of the KKA fractional-order Lassa fever model for selected values of the fractional order α. The panels display the trajectories in the $(S(t), I(t))$, $(M(t), J(t))$, and $(S(t), R(t))$ planes. These plots illustrate the coupled evolution between susceptible and infected humans, susceptible and infected rodents, and susceptible and recovered humans, respectively. The trajectories confirm that decreasing α slows the motion along the phase paths and modifies the transient interaction among the epidemiological compartments through memory effects.

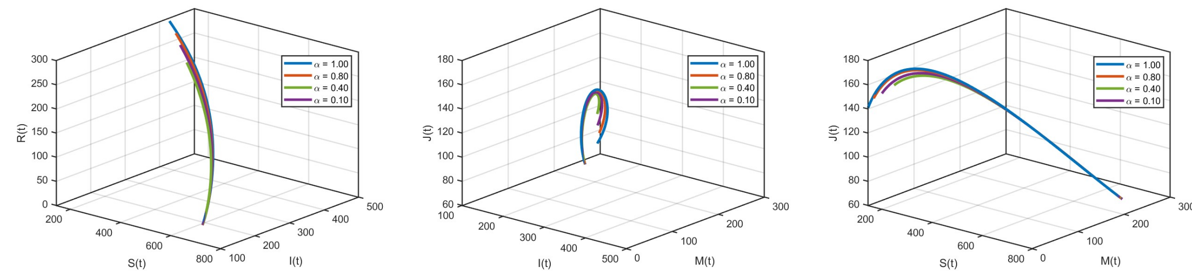

(a) **(b)** **(c)**

Figure 3. Three-dimensional phase portraits of the KKA fractional-order Lassa fever model for selected values of the fractional order α. The panels depict the trajectories in the $(S(t), I(t), R(t))$, $(M(t), I(t), J(t))$, and $(M(t), S(t), J(t))$ spaces, respectively. These plots provide a geometric view of the joint evolution of the human and rodent populations and show that the fractional order α strongly influences the transient spread of the disease, with smaller values of α yielding smoother and slower trajectories due to stronger memory effects.

A more detailed inspection of Figures 1–3 highlights the main numerical findings of the study. In Figure 1, the susceptible human population $S(t)$ and susceptible rodent population $M(t)$ decrease over time, showing the movement of individuals from susceptible classes toward infected or recovered states. The infected human population $I(t)$ and infected rodent population $J(t)$ initially increase, reach peak levels, and then decline, which reflects the outbreak growth and subsequent reduction caused by recovery, mortality, and depletion of susceptible individuals. The recovered class $R(t)$ increases steadily, indicating the accumulation of individuals who leave the infected class through recovery. The comparison of different fractional orders shows that smaller values of α slow the disease progression and delay the infection peaks. This demonstrates that the fractional order controls the strength of memory in the system. Figures 2 and 3 further support these findings from a phase-space point of view. The two-dimensional phase portraits show how the infected human and infected rodent populations evolve jointly with the susceptible and recovered classes. The three-dimensional phase portraits provide a clearer geometric representation of the coupled human–rodent interaction. In all phase plots, decreasing α modifies the path followed by the system and slows its movement along the trajectory. This confirms that the fractional-order model captures memory-dependent transient behavior that is not visible in the classical integer-order case. Therefore, the figures collectively show that the proposed KKA fractional model is able to describe delayed, smooth, and more persistent epidemic evolution.

The numerical results indicate that the fractional order has a substantial effect on the transmission dynamics. In the classical case $\alpha = 1$, the model reduces to the standard integer-order system, and the trajectories recover the usual epidemic behavior. For $0 < \alpha < 1$, the KKA fractional derivative introduces memory effects that modify the transient evolution of all compartments. In particular, decreasing α slows the rate of variation of the state variables, produces smoother trajectories, and delays the progression of the epidemic. As a consequence, the infected human class $I(t)$ and the infected rodent class $J(t)$ increase more gradually, attain their peak values later, and then decline more smoothly when the memory effect is stronger. The main feature revealed by the fractional-order formulation is the memory-dependent transient response of the Lassa fever system. Compared with the integer-order case $\alpha = 1$, the fractional cases $0 < \alpha < 1$ show that past states of the system influence the present evolution of the disease. This effect appears numerically through delayed infection peaks, smoother trajectories, slower changes in the susceptible, infected, recovered, and rodent compartments, and modified phase paths. Hence, the fractional-order model does not merely reproduce the integer-order dynamics; it provides additional information about how memory strength affects the timing, persistence, and gradual evolution of human-rodent disease transmission. Biologically, this pattern indicates that the evolution of the disease is influenced not only by the system's current state but also by its previous states. Hence, the KKA fractional-order formulation provides a more flexible framework for describing the persistence and gradual evolution of Lassa fever transmission than the classical model. Moreover, the numerical profiles remain nonnegative for all simulated time levels, which is consistent with the positivity and boundedness results established earlier.

The simulations also show that the susceptible human population $S(t)$ and the susceptible rodent population $M(t)$ decrease progressively over time, whereas the recovered human population $R(t)$ increases smoothly toward its long-term level. For smaller values of α, these changes occur more slowly, confirming that the fractional order acts as an additional parameter controlling the speed of disease spread and recovery. The phase portraits in Figures 2 and 3 further support this interpretation by showing that smaller values of α slow the motion along the phase paths and modify the transient coupling among the human and rodent classes.

The numerical experiments support the theoretical analysis and demonstrate that the proposed KKA Adams-Bashforth method is effective for simulating the Lassa fever system. The obtained results confirm that the KKA fractional-order model is capable of reproducing biologically meaningful dynamics while revealing how memory influences both the short-term outbreak profile and the long-term evolution of the disease.

The simulations further indicate that the fractional order has a clear influence on the transient behavior of the system. Although the qualitative pattern of each compartment remains unchanged, the speed of increase or decrease and the corresponding population levels vary with α. This confirms that the KKA fractional operator introduces a memory effect into the model, allowing the dynamics to capture nonlocal temporal dependence that cannot be represented by the classical integer-order framework. Hence, the fractional-order formulation provides additional flexibility in describing the spread of Lassa fever and the interaction between the human and rodent populations.

To further examine the numerical behavior of the proposed model, we also investigate the effect of selected epidemiological parameters on the transmission dynamics. In these simulations, one parameter is varied at a time around its baseline value, while all other parameters are kept fixed as in Table 1. This allows us to identify how the main transmission, recovery, and mortality parameters influence the evolution of the infected human and infected rodent populations. The simulations show that increasing the human-to-human transmission rate β_h accelerates the growth of the infected human population and produces a higher infection peak. Similarly, increasing the rodent-to-human transmission rate β_r strengthens the contribution of infected rodents to human infection, leading to a larger outbreak among humans. An increase in the human-to-rodent transmission parameter β_{hr} raises the infected rodent population and can indirectly sustain human infection through the reservoir pathway. In contrast, increasing the recovery rate ϵ reduces the infected human population more rapidly and increases the recovered class earlier. A larger disease-induced death rate δ_h lowers the infected human population through removal by mortality, although it represents a more severe epidemiological outcome. Increasing the waning-immunity rate γ returns more recovered individuals to the susceptible class and may prolong transmission. Moreover, changes in the rodent mortality rate μ_r directly affect the persistence of the rodent reservoir and therefore influence the long-term infection pressure on the human population. These parameter-effect simulations confirm that transmission parameters increase infection levels, whereas recovery and mortality-related parameters reduce or reshape the infected populations. This supports the sensitivity information reported in Table 1 and shows that the proposed KKA Adams-Bashforth scheme can capture both memory effects and parameter-dependent changes in the Lassa fever dynamics. The use of different parameter values provides important epidemiological insight into the proposed Lassa fever model. Varying the transmission parameters allows us to identify how strongly human-to-human, rodent-to-human, and human-to-rodent interactions contribute to disease spread. Larger transmission rates increase the infected human and rodent populations and indicate a higher outbreak potential. In contrast, increasing the recovery rate reduces the infected human population and represents the positive effect of treatment or improved case management. Changes in the waning-immunity rate show how loss of temporary protection may return recovered individuals to the susceptible class and prolong transmission. Similarly, mortality-related parameters affect the persistence of infected classes and the long-term population structure.

To complement the numerical simulations, the computed solutions of the proposed KKA fractional-order Lassa fever model are also used to train a deep neural network surrogate. The aim of this surrogate is to learn the mapping between the model input and the corresponding state trajectories, so that repeated evaluations of the dynamical system can be carried out more efficiently. In the present study, a single deep neural network is trained for all state variables and all considered fractional orders.

The training performance and diagnostic results are shown in Figure 4. Figure 4(a) presents the mean squared error curves for the training, validation, and testing datasets. The training and validation errors decrease steadily throughout the learning process, and the best validation performance is attained at epoch 300 with a value of 4.1467×10^{-7}. Although the testing curve remains higher than the training and validation curves, the overall behavior still indicates that the network successfully captures the dominant structure of the numerical data. Figure 4(b) shows the training-state plots, where the gradient reaches 2.3282×10^{-6}, the damping parameter is $\mu = 10^{-8}$, and the validation checks remain at 0 at epoch 300, all of which are consistent with stable convergence of the optimization procedure. Figure 4(c) displays the error histogram, in which the residuals are strongly concentrated around zero, indicating that most prediction errors are small. The regression plots in Figure 4(d) further confirm the predictive quality of the network, with correlation coefficients $R = 1.0000$ for training, $R = 1.0000$ for validation, $R = 0.97463$ for testing, and $R = 0.99742$ overall. Finally, Figure 4(e) shows the function-fitting and residual plots for a representative output element. The close agreement between the target and predicted values, together with the small residuals, demonstrates that the trained network reproduces the numerical trajectories of the proposed KKA Lassa fever system with high accuracy.

The numerical experiments and the deep learning diagnostics together verify that the proposed model is capable of producing stable and biologically consistent dynamics, while the neural network surrogate provides an efficient and accurate computational tool for approximation, calibration, and further predictive analysis.

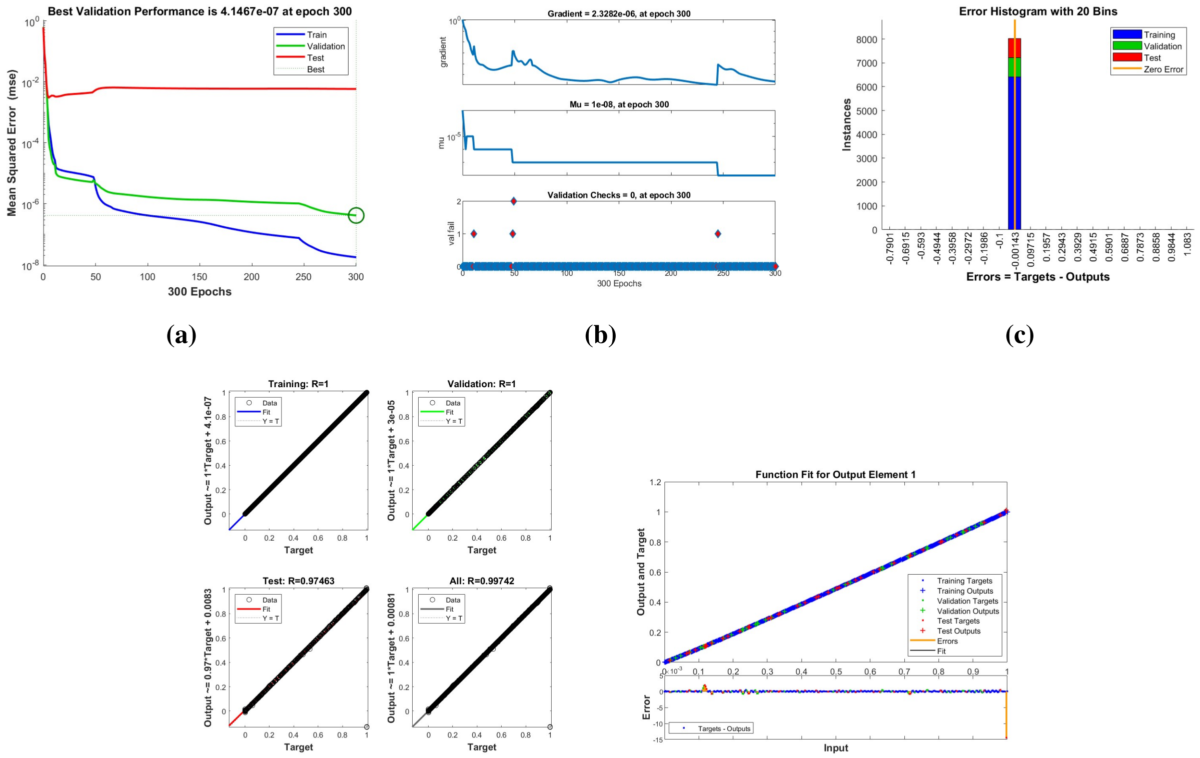

(a) (b) (c)

(d) (e)

Figure 4. Training diagnostics of the single deep neural network surrogate for the proposed KKA fractional-order Lassa fever model: (a) mean squared error performance for the training, validation, and testing datasets, with best validation performance 4.1467×10^{-7} at epoch 300; (b) training-state plots showing the gradient, damping parameter, and validation checks; (c) error histogram of the residuals; (d) regression plots for the training, validation, testing, and overall datasets; and (e) function-fitting and residual plots for a representative output element.

6. Parameter estimation

Although the proposed KKA fractional-order Lassa fever model is analyzed theoretically and simulated numerically using the baseline values in Table 1, some transmission-related quantities are not directly measurable in practice. For this reason, parameter estimation is carried out in order to examine whether the model can recover important epidemiological parameters from trajectory data and to assess the consistency of the fitted dynamics with the reference solutions. In this section, we calibrate a selected subset of parameters while keeping the remaining parameters fixed at the baseline values reported in Table 1.

Let $t_1, t_2, \ldots, t_n$ denote the observation times and let $Y_i = (I^{\text{obs}}(t_i), J^{\text{obs}}(t_i))^\top, i = 1, 2, \ldots, n$, represent the available observed data. Since real data are not used in the present study, the observations are generated synthetically from the numerical solution of the proposed fractional-order Lassa fever system. More precisely, the clean reference trajectories are first obtained from the KKA Adams–Bashforth scheme, after which perturbed data are constructed to mimic measurement uncertainty. The calibration is then performed by minimizing the discrepancy between the observed infected-human and infected-rodent trajectories and the corresponding model outputs.

In particular, we estimate the parameter vector $\Theta = (\beta_h, \beta_r, \beta_{hr}, I(0), J(0))$, where β_h denotes the contribution of infected humans to the human force of infection, β_r is the transmission contribution from infected rodents to humans, β_{hr} is the human-to-rodent transmission parameter, and $I(0)$ and $J(0)$ are the initial infected human and infected rodent populations, respectively. These quantities are selected because they play a central role in the coupled human-rodent transmission process and have a direct influence on the transient epidemic profiles. The remaining parameters, together with the other initial conditions, are fixed at their nominal values.

The unknown vector Θ is obtained from the nonlinear least-squares problem $\Theta^* = \arg\min_{\Theta\in\Omega} J(\Theta)$, where

$$J(\Theta) = \sum_{i=1}^{n} \left\| \begin{pmatrix} I(t_i;\Theta) \\ J(t_i;\Theta) \end{pmatrix} - \begin{pmatrix} I^{\mathrm{obs}}(t_i) \\ J^{\mathrm{obs}}(t_i) \end{pmatrix} \right\|^2 .$$

Here, $I(t_i;\Theta)$ and $J(t_i;\Theta)$ denote the model-predicted infected human and infected rodent populations at time t_i, respectively, and Ω is the biologically admissible parameter set. In the present framework, the admissible region is chosen so that all estimated parameters remain nonnegative and epidemiologically meaningful throughout the calibration process.

To evaluate the robustness of the estimation procedure, two calibration settings are considered. In the first case, the fitting is examined against clean synthetic trajectories generated by the KKA fractional model. In the second case, noisy synthetic observations are used in order to imitate perturbations that typically arise in epidemiological measurements. After estimating the unknown quantities, the fitted parameter set is inserted back into the full Lassa fever system so that the reconstructed trajectories of all five compartments can be compared with the corresponding reference solutions.

Figure 5 shows the comparison between the synthetic true trajectories and the fitted trajectories for the five state variables $S(t)$, $I(t)$, $R(t)$, $M(t)$, and $J(t)$. The fitted curves closely follow the reference solutions in all compartments, indicating that the estimation procedure is able to recover the dominant dynamical behavior of the model. In particular, the agreement in the infected human and infected rodent classes confirms that the calibrated transmission parameters capture the main features of the coupled host–reservoir interaction.

Figure 6 presents the fitting results when noisy synthetic observations are used. Although the perturbed data exhibit visible fluctuations around the underlying epidemic trends, the fitted trajectories still reproduce the principal temporal patterns of all compartments. This indicates that the proposed calibration framework remains stable under moderate measurement noise and is able to extract meaningful information from perturbed data. To further assess the global quality of the reconstruction, Figure 7 displays heatmaps of the normalized clean trajectories, normalized fitted trajectories, and normalized absolute error. The first two heatmaps exhibit very similar temporal structures across the five compartments, while the absolute-error heatmap remains at relatively low levels over most of the observation window. This visual agreement provides additional evidence that the estimated parameter set yields a reliable approximation of the reference Lassa fever dynamics.

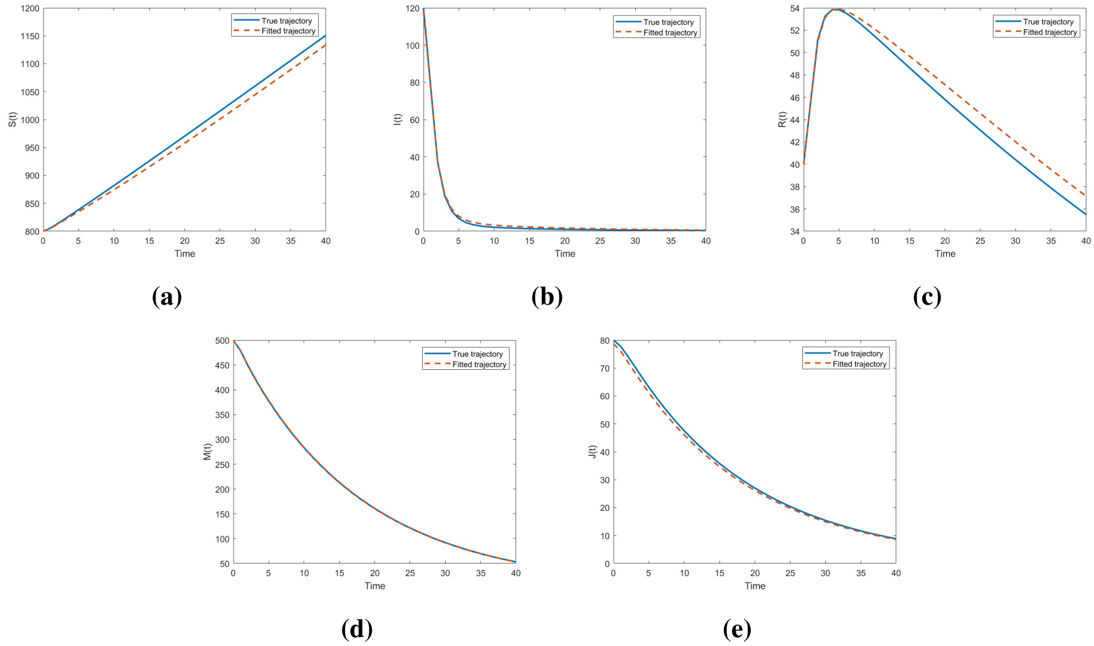

Figure 5. Comparison between the synthetic true trajectories and the fitted trajectories for the state variables of the proposed KKA fractional-order Lassa fever model: (a) $S(t)$, (b) $I(t)$, (c) $R(t)$, (d) $M(t)$, and (e) $J(t)$. The close agreement between the reference and fitted solutions shows that the calibration procedure accurately reproduces the main dynamical behavior of the human–rodent system.

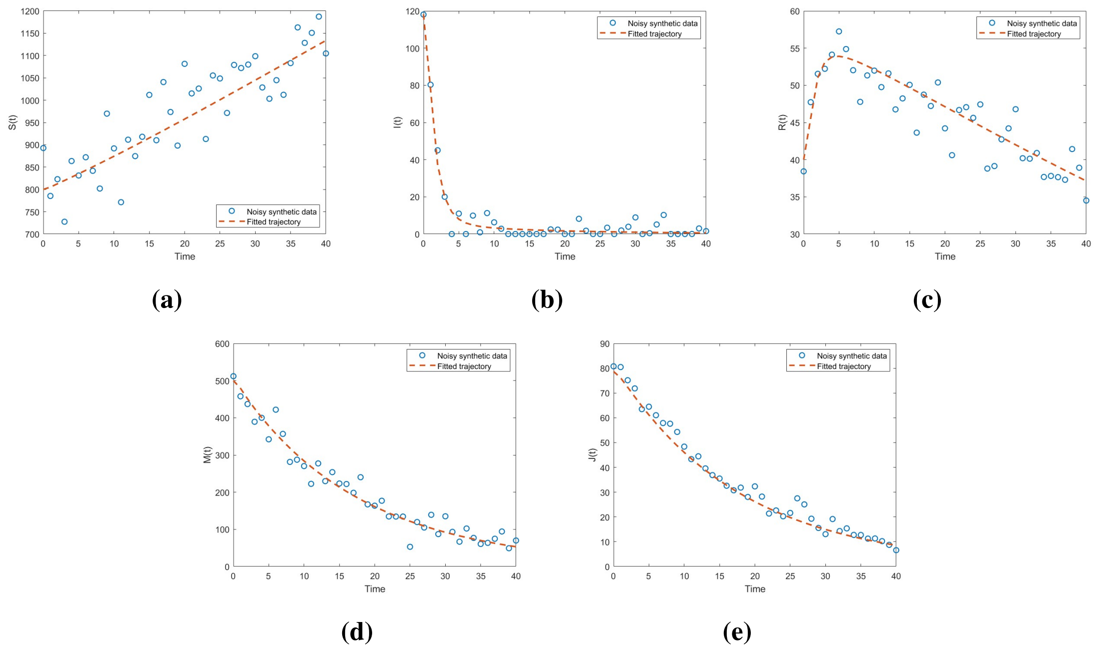

Figure 6. Comparison between noisy synthetic observations and the fitted trajectories for the state variables of the proposed KKA fractional-order Lassa fever model: (a) $S(t)$, (b) $I(t)$, (c) $R(t)$, (d) $M(t)$, and (e) $J(t)$. The fitted trajectories maintain the model's key temporal patterns despite data perturbations, indicating robust estimation.

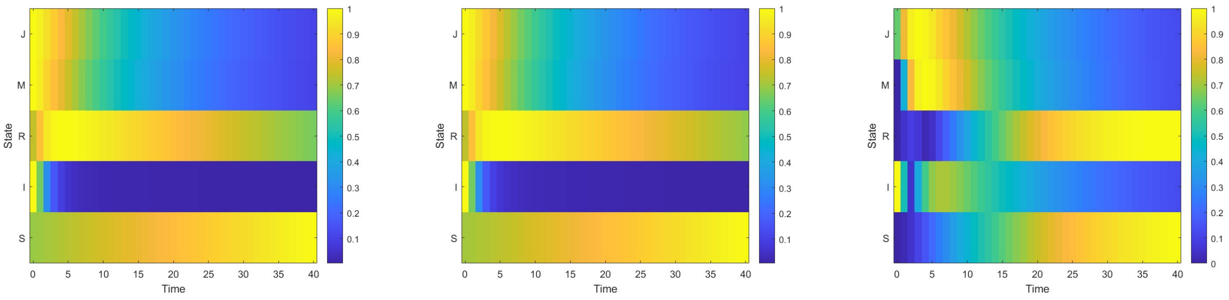

(a) **(b)** **(c)**

Figure 7. Heatmap representation of the trajectory patterns for the proposed KKA fractional-order Lassa fever model: (a) normalized clean trajectories, (b) normalized fitted trajectories, and (c) normalized absolute error. The strong similarity between the first two heatmaps and the low error levels in the third panel confirm the consistency of the calibrated dynamics.

Figures 4–7 confirm the computational reliability of the proposed framework. Figure 4 shows that the deep neural network surrogate learns the numerical trajectories with small errors and strong regression performance. Figures 5 and 6 demonstrate that the fitted trajectories remain close to the reference solutions under both clean and noisy synthetic data. Figure 7 gives a global visual comparison through heatmaps, where the similarity between the clean and fitted trajectories and the low absolute error confirm the consistency of the calibrated model. These results indicate that the proposed fractional-order model is not only theoretically well-posed and numerically stable, but also suitable for data-driven approximation and parameter-recovery studies. The results of this section show that the proposed parameter-estimation procedure is effective for the KKA fractional-order Lassa fever model. The fitted solutions remain in good agreement with both clean and noisy synthetic data, and the heatmap comparison confirms the consistency between the reference and reconstructed trajectories. These results support the use of the model for future calibration studies, inverse problems, and data-driven extensions of Lassa fever dynamics.

7. Conclusions

This paper presented a fractional-order Lassa fever model in the Caputo-type KKA framework to account for memory effects in coupled human-rodent transmission. The model consists of five epidemiological compartments and was rewritten in an equivalent Volterra-type integral form by using the inverse relation between the KKA derivative and its associated integral. The analysis established positivity, boundedness, existence, uniqueness, and Ulam-Hyers stability, confirming that the model is biologically meaningful and mathematically well-posed. For the numerical study, a two-step KKA Adams-Bashforth scheme was developed and applied to the system. The proposed numerical scheme has several advantages in the present setting. Unlike standard integer-order schemes, it is constructed directly from the Volterra-type integral representation of the KKA fractional model and therefore includes the memory contribution of the fractional operator. Compared with simple one-step approaches, the two-step Adams-Bashforth structure provides a more accurate explicit approximation while keeping the implementation relatively simple. The method is also written componentwise for all state variables, making it convenient for simulating coupled human-rodent disease dynamics. In addition, the scheme remains consistent with the fractional formulation and allows the classical integer-order case to be recovered when $\alpha = 1$. Therefore, the proposed method is suitable for examining how different fractional orders affect the transient behavior of the Lassa fever model. The simulations showed that the fractional order strongly influences the disease dynamics, with smaller values of α producing stronger memory effects and slower epidemic evolution, while $\alpha = 1$ recovers the classical case. A deep neural network surrogate was also trained on the numerical trajectories and showed strong predictive accuracy. In addition, the parameter-estimation study using clean and noisy synthetic data demonstrated good agreement between fitted and reference solutions. More specifically, the numerical results showed that the susceptible human and rodent populations decrease with time, while the infected human and infected rodent populations first increase to peak levels and then decline. The recovered human class increases steadily, reflecting the transfer of infected individuals into the recovered compartment. The comparison of different fractional orders confirmed that smaller values of α delay the infection peaks, smooth the solution curves, and slow the movement of the trajectories in the phase portraits. These results demonstrate the ability of the KKA fractional model to capture memory-dependent epidemic behavior. The neural-network results also supported the computational performance of the proposed framework, with the training, validation, and testing errors decreasing to very small levels and the regression plots showing strong agreement between predicted and target trajectories. Furthermore, the parameter-estimation results showed that the fitted solutions closely followed both clean and noisy synthetic data, while the heatmap comparison indicated low reconstruction error. Thus, the calculated results confirm the reliability of the numerical method, the predictive capability of the neural-network surrogate, and the robustness of the parameter-estimation procedure. These findings show that the fractional-order approach reveals memory-driven delay, smoothing, and slower epidemic progression, which are not visible in the classical integer-order model. The proposed framework provides a useful basis for future research on real-data fitting, inverse problems, optimal control, and extended epidemic models with spatial, stochastic, or data-driven features.

Author contributions

Ramsha Shafqat: Conceptualization, Methodology, Software, Investigation, Resources, Writing–original draft, Writing–review and editing; Mohammed M. Alshamrani: Formal analysis, Resources, Supervision, Project administration, Funding acquisition. All authors have read and approved the final version of the manuscript for publication.

Use of Generative-AI tools declaration

The authors declare that they have not used Artificial Intelligence (AI) tools in the creation of this article.

Acknowledgments

The authors would like to acknowledge the Deanship of Graduate Studies and Scientific Research, Taif University for funding this work.

Conflict of interest

All authors declare no conflicts of interest in this paper.

References

1. K. O. Achema, D. J. Yayaha, W. T. Ademosu, Mathematical model formulation and analysis of the transmission dynamics of Lassa fever, *Ann. Commun. Math.*, **9** (2026), 9. https://doi.org/10.62072/acm.2026.09009
2. J. U. A. Grace, I. J. Egoh, N. Udensi, Epidemiological trends of Lassa fever in Nigeria from 2015–2021: A review, *Therapeut. Adv. Infect. Dis.*, **8** (2021), 20499361211058252. https://doi.org/10.1177/20499361211058252
3. A. Musa, K. Osuolale, D. Lawal, A. Salako, F. Aponinuola, W. Tijani, et al., Modelling seasonal variation and Lassa fever outbreak in Nigeria: A predictive approach, *Int. J. Data Sci. Anal.*, **10** (2024), 100–108. https://doi.org/10.11648/j.ijdsa.20241005.12
4. E. A. Bakare, E. B. Are, O. E. Abolarin, S. A. Osanyinlusi, B. Ngwu, O. N. Ubaka, Mathematical modelling and analysis of transmission dynamics of Lassa fever, *J. Appl. Math.*, **2020** (2020), 6131708. https://doi.org/10.1155/2020/6131708
5. I. O. Abiola, A. S. Oyewole, T. T. Yusuf, Mathematical modelling of Lassa-fever transmission dynamics with optimal control of selected control measures, *Model. Earth Syst. Environ.*, **10** (2024), 7443–7458. https://doi.org/10.1007/s40808-024-02168-z
6. S. S. Musa, S. Zhao, D. Gao, Q. Lin, G. Chowell, D. He, Mechanistic modelling of the large-scale Lassa fever epidemics in Nigeria from 2016 to 2019, *J. Theor. Biol.*, **493** (2020), 110209. https://doi.org/10.1016/j.jtbi.2020.110209
7. A. A. Ayoade, O. Aliu, O. Taiye, The effect of treatment compliance on the dynamics and control of Lassa fever: An insight from mathematical modeling, *SeMA J.*, **82** (2025), 89–108. https://doi.org/10.1007/s40324-024-00353-9
8. S. Dachollom, C. E. Madubueze, Mathematical model of the transmission dynamics of Lassa fever infection with controls, *Math. Model. Appl.*, **5** (2020), 65–86. https://doi.org/10.11648/j.mma.20200502.13
9. A. El-Mesady, T. M. Al-shami, H. M. Ali, Optimal control efforts to reduce the transmission of HPV in a fractional-order mathematical model, *Boundary Value Probl.*, **2025** (2025), 42. https://doi.org/10.1186/s13661-024-01991-8
10. A. Elsonbaty, T. M. Al-Shami, A. El-Mesady, Unveiling the dynamics of meningitis infections: A comprehensive study of a novel fractional-order model with optimal control strategies, *Boundary Value Probl.*, **2025** (2025), 48. https://doi.org/10.1186/s13661-025-02034-6
11. R. Shafqat, M. M. Alshamrani, Deep learning for parameter estimation in a typhoid fever model, *AIMS Math.*, **11** (2026), 14984–15007. https://doi.org/10.3934/math.2026616
12. R. Shafqat, A. Alsaadi, A hybrid predictive framework for Zika dynamics using the normalized Caputo-Fabrizio operator, *J. Math.*, **2026** (2026), 4681248. https://doi.org/10.1155/jom/4681248

13. A. Al-Quran, R. Shafqat, A. Alsaadi, A. M. Djaouti, Well-posedness and Ulam-Hyers stability of a normalized Caputo-Fabrizio fractional model for ischemic heart disease progression, *J. Math.*, **2026** (2026), 9509503. https://doi.org/10.1155/jom/9509503

14. R. Shafqat, A. Al-Quran, A. Alsaadi, A. M. Djaouti, Normalized Caputo-Fabrizio SVIR modeling and bifurcation analysis, *Sci. Rep.*, **1**, (2026), 8193. https://doi.org/10.1038/s41598-026-38301-4

15. D. Kayo, A. Akgül, Adams-Bashforth scheme and Kayo-Kengne-Akgül derivative: Connexion and chaotic modelling, *Univ. J. Math. Appl.*, **9** (2026), 53–63. https://doi.org/10.32323/ujma.1879909